The role of mitotype variation and positive epistasis in trait differences between *Saccharomyces* species

Jun-Ting Johnson Wang[1,2], Ping Ling Priscilla Ng[1,3], Maceo E. Powers[1,4], Catherine H. Rha[1], Rachel B. Brem[1*]

[1]Department of Plant and Microbial Biology, University of California, Berkeley, Berkeley, CA, 94720

[2]Graduate Group in Comparative Biochemistry, University of California, Berkeley, Berkeley, CA, 94720

[3]Current address: BillionToOne, Menlo Park, CA, 94025

[4]Current address: Laboratory of Viral Diseases, National Institute of Allergy and Infectious Diseases, National Institutes of Health, Bethesda, MD, 20892

*To whom correspondence should be addressed (rbrem@berkeley.edu)

Abstract

Many traits of interest in biology evolved long ago and are fixed in a particular species, distinguishing it from other sister taxa. Elucidating the mechanisms underlying such divergences across reproductive barriers has been a key challenge for evolutionary biologists. The yeast *Saccharomyces cerevisiae* is unique among its relatives for its ability to thrive at high temperature. The genetic determinants of the trait remain incompletely understood, and we sought to understand the role in its architecture of species variation in mitochondrial DNA. We used mitochondrial transgenesis to show that *S. cerevisiae* mitotypes were sufficient for a partial boost to thermotolerance and respiration in the *S. paradoxus* background. These mitochondrial alleles worked best when the background also harbored a pro-thermotolerance nuclear genotype, attesting to positive epistasis between the two genomes. The benefits of *S. cerevisiae* alleles in terms of respiration and growth at high temperature came at the cost of worse performance in cooler conditions. Together, our results establish this system as a case in which mitoalleles drive fitness benefits in a manner compatible with, and fostered by, the nuclear genome.

Introduction

A central aim in evolutionary genetics is to figure out how organisms acquire new traits. In the study of within-species variation, a rich literature has provided insights into the mechanisms of local adaptation in the wild (Elena 2017; Kraemer and Boynton 2017; Sork 2017; Rees et al. 2020; Bazzicalupo 2022). Yet many characters of basic and applied interest evolved long ago and are fixed in a particular species, distinguishing it from unaffected relatives. Against a backdrop of years of genomic and experimental pursuit (Allen Orr 2001; Nikolov and Tsiantis 2015; Weiss and Brem 2019), the genetic principles governing trait divergence over long timescales remain poorly understood, with the widest knowledge gap in the case of polygenic architectures. Indeed, an adaptive trait that arose long ago, and ultimately fixed in a given species, could have undergone millions of years of refinement, and could have a genetic architecture governed by principles quite different from recently-arisen intra-species trait polymorphism that is the focus of much of the field. Shedding light on these mechanisms, by dissecting the genetics of adaptations between isolated taxa, remains a key challenge.

Sequence divergence in mitotype, the DNA of the mitochondrial organelle, have emerged as an important driver of naturally varying traits. Mitotype variants have been directly implicated in trait diversity, both independently and in concert with nuclear genomes, in a rich literature focused on polymorphism within species (Melvin and Ballard 2006; Tranah 2011; Houtkooper et al. 2013; Sullivan and Chandel 2014; Mossman et al. 2016 Nov 14; Mossman et al. 2016; Patel et al. 2016; Camus et al. 2017; Camus and Dowling 2018; Mossman et al. 2019; Sun et al. 2019; Camus et al. 2020; Salminen and Vale 2020; Anderson et al. 2022; Cao et al. 2022; Meng et al. 2022; Oppong et al. 2022; Quéméneur et al. 2022; Parra et al. 2023; Moran et al. 2024). Though small in length, the mitochondrial genome has the potential for an outsize influence on trait variation, given its increased mutation rate and large mutational target of the multi-copy mitochondrial genome relative to nuclear chromosomes (Pakendorf and Stoneking 2005; Chou and Leu 2015; Ferreira and Rodriguez 2024).

Saccharomyces budding yeasts diverged from a common ancestor ~20 million years ago (Kellis et al. 2003) and have served for decades as a model for the study of interspecific trait variation, including in metabolism, genome content, cell cycle, and reproductive isolation (Hou et al. 2014; Roop et al. 2016; Bozdag et al. 2021; Fredericks et al. 2021; Lupo et al. 2021; Marsit et al. 2021; Smukowski Heil et al. 2021; Swamy et al. 2022; Crandall et al. 2023; Forejt and Jansa 2023; Peris et al. 2023). A long-standing subset of this field has focused on species-unique traits

driven by mitochondrial genomes (Sulo et al. 2003; Wolff et al. 2014; De Chiara et al. 2020; Hewitt et al. 2020; Hénault et al. 2022), with particularly detailed mechanistic validation in studies of speciation (Lee et al. 2008; Chou et al. 2010; Mário et al. 2015; Jhuang et al. 2017) (complementing studies of mitotype polymorphism within yeast species (Wolters et al. 2015; Leducq et al. 2017; Wolters et al. 2018; Vijayraghavan et al. 2019; Vijayraghavan et al. 2019; Nguyen et al. 2020)). A key model trait in the *Saccharomyces* system is temperature preference, as the best-studied yeast species, *S. cerevisiae,* is unique within the *Saccharomyces* clade for its ability to thrive at high temperature (Sweeney et al. 2004; Gonçalves et al. 2011; Salvadó et al. 2011), whereas others in the clade exhibit cryotolerance (Paget et al. 2014; Pinto et al. 2025). Species-level variation in these traits has been inaccessible to analysis by classic methods like GWAS or linkage mapping, which rely on recombinants in fertile crosses. For this reason, mechanisms by which nature built thermotolerance in *S. cerevisiae* from a thermosensitive ancestor were difficult to access for the classic literature. But the system represents a testbed for alternative approaches for genetic dissection across species boundaries, which have fostered insight into the architectures of species differences in thermotolerance and their adaptive history (Weiss et al. 2018; AlZaben et al. 2021; Walunjkar et al. 2025) and cold tolerance (Paget et al. 2014; Pinto et al. 2025). The contribution of mitochondrial genome variation to this trait has also been suggested, based on analyses of interspecies hybrids (Baker et al. 2019; Li et al. 2019; Hewitt et al. 2020); exactly what the divergent mitotypes of *Saccharomyces* species do phenotypically, and how they exert their effects, remains incompletely understood.

We set out to pursue in more depth the phenotypic impact of mitochondrial variation between *Saccharomyces* species, both in isolation and in conjunction with nuclear loci. We anticipated that our findings would further illuminate the mechanisms of thermotolerance and their evolutionary history. We designed an approach that used *S. paradoxus*, a relatively thermosensitive species sister to *S. cerevisiae,* as a foreign background for manipulations of the nuclear and mitochondrial genomes, to investigate their functions and their interactions.

Results

S. cerevisiae* mitotypes are sufficient to heighten respiratory behaviors in *S. paradoxus

Previous studies have used yeast interspecies hybrids to establish an association between *S. cerevisiae* mitochondrial alleles and thermotolerance (Baker et al. 2019; Li et al. 2019; Hewitt et al. 2020), which parallels the advantage of *S. cerevisiae* purebreds at high temperature, relative to other species in the clade. We reasoned that investigating mitotype genetics in purebred *S. paradoxus* could help shed additional light on the mechanisms of evolutionary innovation along the *S. cerevisiae* lineage. For this purpose, we developed a series of cybrids, in which we introduced each mitochondrial genome in turn from a suite of *S. cerevisiae* isolates from different geographical locations, which all grew well in standard conditions and at high temperature (Figure S1), into a tester strain of *S. paradoxus*, the English oak tree isolate Z1 (Figure 1). Since they lack the endogenous *S. paradoxus* mitotype, these strains represented an experimental resource for the study of the phenotypic impact of *S. cerevisiae* mitochondrial alleles in an isogenic background, and they were viable and stable as expected (Sulo et al. 2003; Mário et al. 2015).

Before using our cybrids to address thermotolerance *per se*, we first investigated the hypothesis that respiration, as a proximal function of the mitochondrion and its genome, would be perturbed by species variation in mitotype. Wild-type *S. cerevisiae* strains as a rule grow better than those of *S. paradoxus* on glycerol, a non-fermentable carbon source (Figure S2), and in interspecies hybrid backgrounds, *S. cerevisiae* mitotypes promote growth in this condition (Li et al. 2019). To

106 explore the impact of *S. cerevisiae* mitochondrial DNA alleles on respiratory growth in a
107 purebred context, we assayed growth of our cybrids in liquid glycerol medium. The results
108 revealed robust improvement attributable to *S. cerevisiae* mitotypes in the *S. paradoxus*
109 background, for three of our *S. cerevisiae* donors (Figure 2A and Fig S3). The fourth cybrid,
110 harboring mitochondrial DNA from the *S. cerevisiae* vineyard isolate Y55, had a defect in growth
111 on glycerol (Figure 2A), which echoes previously reported incompatibilities of this mitotype in
112 other backgrounds (Wolters et al. 2018). Together, these data suggested that pro-respiratory
113 effects could be a prevalent characteristic of mitochondrial genomes from across the *S.*
114 *cerevisiae* population.

115 As a more direct measure of metabolic effects driven by *S. cerevisiae* mitochondria DNA, we
116 established an assay of reduction of the colorimetric substrate 1-(4,5-dimethylthiazol-2-yl)-3,5-
117 diphenyltetrazolium bromide (MTT) in glucose medium. This signal serves as a reporter of
118 activities of the electron transport chain, particularly succinate dehydrogenase (Slater et al.
119 1963; Sánchez and Königsberg 2006; Jain et al. 2018) (though see (Shoemaker et al. 2004)
120 and (Peng et al. 2005)), and thus is informative as a marker of respiration. A first set of
121 observations revealed no detectable impact of mitotype on MTT reduction during culture in
122 liquid glucose medium at 28°C in the *S. paradoxus* background (Figure 3A and Fig S4A). We
123 reasoned that the metabolic effect of *S. cerevisiae* mitotypes might be better resolved at higher
124 temperatures, in which yeast cells respire particularly avidly (Rikhvanov et al. 2001). Consistent
125 with this notion, in culture at 39°C in glucose medium, we observed increased MTT reduction in
126 all cybrids except for that harboring *S. cerevisiae* Y55 mitochondrial DNA, relative to wild-type
127 Z1 *S. paradoxus* with its endogenous mitochondrial genome (Figure 3B and Fig S4B). Together,
128 these results established that in the *S. paradoxus* background, *S. cerevisiae* mitotypes can be
129 sufficient for increased growth and metabolic behaviors that are signatures of respiration.

130 **_S. cerevisiae_ mitotypes boost thermotolerance in _S. paradoxus_**

131 We now turned to high-temperature growth proper, as an additional phenotype that we
132 hypothesized would be modulated by mitotype in our yeast species comparison. To test the
133 latter prediction, we measured cell density during growth in liquid glucose medium at 39°C, for
134 each of our cybrid strains harboring *S. cerevisiae* mitochondrial DNA in Z1 *S. paradoxus*.
135 Results revealed a 10% to 70% improvement in accumulated biomass in this assay, relative to
136 wild-type *S. paradoxus,* in all cybrids except the one for which *S. cerevisiae* Y55 was the
137 mitochondrial donor (Figure 2A). In an expanded panel of cybrids using additional *S. cerevisiae*
138 mitotype donors, a boost in thermotolerance was also apparent in all cases (Figure S5). Thus,
139 *S. cerevisiae* mitotypes were sufficient to confer thermotolerance benefits, in some cases
140 sizeable ones, in *S. paradoxus*. Controls established that *S. cerevisiae* mitotypes had
141 phenotypic effects in a fixed *S. cerevisiae* background mirroring those in *S. paradoxus*, though
142 no *S. cerevisiae* cybrid exceeded the thermotolerance of the wild-type of this species (Figure
143 S6). Interestingly, after 24 hours of incubation at 39°C, cultures of cybrids in the *S. paradoxus*
144 background harbored very few viable cells (Figure S7). We conclude that in such cybrids, *S.*
145 *cerevisiae* mitochondrial DNAs enable additional cell divisions during high-temperature
146 exposure, after which failures of factors encoded by the *S. paradoxus* nuclear genome
147 ultimately prevent further growth and kill cells outright.

148 Thermotolerance phenotypes as they varied across our panel of *S. paradoxus* cybrids
149 correlated tightly with the respiratory behaviors we had documented in assays of growth in non-
150 fermentable carbon sources in these strains (Figures 2A and 2B) and MTT reduction (Figure 3).
151 That is, among *S. paradoxus* cybrids, those performing best in respiratory contexts were the
152 most thermotolerant, and the worst in respiratory assays grew the worst at high temperature.
153 These results are most consistent with a causal relationship between the traits, whereby the *S.*

154 *cerevisiae* mitotypes that foster better thermotolerance do it by improving respiration—a
155 metabolic underpinning for the capacity to grow under high-temperature challenge.

156 **Antagonistic pleiotropy by *S. cerevisiae* mitotypes in temperate conditions and ethanol**

157 Previous studies using interspecies hybrids have reported a defect in cold temperatures
158 attributable to *S. cerevisiae* mitotypes relative to those of *S. paradoxus* or other relatives (Baker
159 et al. 2019; Li et al. 2019; Hewitt et al. 2020). To test whether such effects would be
160 recapitulated in purebred backgrounds, in Z1 *S. paradoxus* derivatives carrying *S. cerevisiae*
161 mitochondrial DNA, we assayed the carrying capacity after culture 23°C in liquid glucose
162 medium, for comparison against a 28°C control and the high-temperature condition (39°C), also
163 with glucose as a carbon source. The results revealed compromised cell density at 23°C in the
164 cybrids that performed the best at high temperature (Figure 2A). This set up an almost perfect
165 anticorrelation between 23°C growth and thermotolerance across strains (Figure 2C), mirroring
166 the observation we had made with respiratory behaviors (Figures 2 and 3). We conclude that *S.*
167 *cerevisiae* mitotypes have specialized to heat stress at the expense of performance at lower
168 temperatures, suggestive of fine-tuning by evolution of the temperature optima of respiratory
169 reactions encoded by the mitochondrial genome.

170 We also noted an anticorrelation across our cybrids between thermotolerance and cell density in
171 glucose at 28°C: at the latter temperature, the most thermotolerant strains harboring *S.*
172 *cerevisiae* DNA performed the worst (Figure 2A). To explore potential drivers of this pattern, we
173 also assayed cell density at 28°C in medium with ethanol as the carbon source, in which we
174 observed most cybrids carrying *S. cerevisiae* mitochondrial DNA to be at a disadvantage (Figure
175 2A). Growth patterns among strains at 28°C and in ethanol were robustly correlated (Figure 2D),
176 suggestive of a mechanistic relationship between them, as expected given that *Saccharomyces*
177 species catabolize ethanol late in the growth cycle after having secreted it (Piskur et al. 2006).
178 In summary, based on our growth and respiration profiles, we conclude that *S. cerevisiae*
179 mitochondrial genomes are drivers of a phenotypic syndrome that includes advantages in most
180 facets of respiration as well as high-temperature growth, and disadvantages at cooler
181 temperatures and during ethanol utilization.

182 **Positive epistasis between mitochondria and nuclear genomes in terms of**
183 **thermotolerance**

184 During the evolution of *S. cerevisiae* as a species, the pro-thermotolerance mitotypes we study
185 here would have arisen alongside changes in nuclear genes which could modify their effects.
186 We sought to shed light on these relationships by modeling them in the *S. paradoxus*
187 background. To this end, we introduced *S. cerevisiae* mitochondrial genomes into a derivative of
188 *S. paradoxus* Z1 that also harbored the alleles from the DBVPG1373 Dutch soil strain of *S.*
189 *cerevisiae* at eight nuclear loci which contribute to thermotolerance (*AFG2, APC1, CEP3, DYN1,*
190 *ESP1, MYO1, SCC2*, and *TAF2*, most of which encode cell division factors; (AlZaben et al.
191 2021)). In assays of cell density at 39°C, the combination of *S. cerevisiae* alleles in the nuclear
192 and mitochondrial genomes together conferred a two-fold improvement relative to wild-type *S.*
193 *paradoxus* (Figure 4, gray bars). This represented an increase in cell divisions early in the
194 treatment, as no cybrids harboring *S. cerevisiae* nuclear alleles maintained viability after 24
195 hours at 39°C (Figure S8), paralleling results from cybrids in the wild-type *S. paradoxus* nuclear
196 background (Figure S7). Advantages in cell density at 39°C manifested regardless of the origin
197 of the mitotype: mitochondrial DNA from across our panel of *S. cerevisiae* strain donors yielded
198 identical high-temperature growth in *S. paradoxus* in the presence of the nuclear
199 thermotolerance genes from *S. cerevisiae,* including the Y55 mitotype that had compromised
200 the phenotype in wild-type *S. paradoxus* (Figures 2A and 4). Thus, the latter incompatibility was
201 resolved by *S. cerevisiae* alleles at our focal nuclear genes.

Also evident from our nuclear-mitochondrial transgenic strain panel was a pattern of positive epistasis. That is, the impact of each *S. cerevisiae* mitotype on thermotolerance was greater in the *S. paradoxus* derivative also harboring nuclear alleles from *S. cerevisiae* than in otherwise wild-type *S. paradoxus* (Figure 4; compare gray and black bars). Mitochondrial DNA from distinct *S. cerevisiae* donors, including Y55, all achieved peak performance at high temperature in the presence of *S. cerevisiae* nuclear genes; no such dependence was detectable in 28°C cultures (Figure S9). That said, the *S. cerevisiae* mitotype that promoted thermotolerance most strongly on its own in the *S. paradoxus* background, from DBVPG1373, benefited the least from the addition of DBVPG1373 alleles of nuclear genes (Figure 4, magenta). Relative to this transgenic, strains harboring other *S. cerevisiae* mitotypes, which had less impact on their own, achieved the same cell density at 39°C in the presence of DBVPG1373 nuclear alleles (Figure 4, blue, green, and orange). These results are most consistent with a ceiling beyond which any *S. cerevisiae* alleles of the mitochondrial genome, even when combined with *S. cerevisiae* alleles of our eight focal nuclear genes, are unable to improve thermotolerance, in the face of defects accruing from other *S. paradoxus* loci. Nonetheless, our data make clear that pro-thermotolerance alleles of mitochondrial DNAs and nuclear genes from *S. cerevisiae* together contribute to the phenotype in a manner that exceeds the sum of their parts.

Discussion

A key goal of comparative genetics is to understand how evolution builds traits over long timescales. In this work, we have leveraged tractable *Saccharomyces* as a testbed for the study of interspecies trait genetics and evolution focused on the mitochondrial genome. Given the evidence that *S. cerevisiae* thermotolerance is the product of positive selection (Weiss et al. 2018; Abrams et al. 2021), it serves as a powerful model of the evolutionary genetics of adaptation over deep divergences. Our findings complement previous studies of mitotype effects in this system (Baker et al. 2019; Li et al. 2019; Hewitt et al. 2020) by tracing the phenotypes conferred by *S. cerevisiae* mitochondrial alleles in purebred backgrounds, including their genetic dependencies.

Our results shed new light on the genetic architecture and evolution of yeast thermotolerance. Our finding of a 70% boost in the trait by an *S. cerevisiae* mitotype outstrips the effect of any one of the nuclear loci previously reported in this system (Weiss et al. 2018). Sequence analyses revealed amino acid alleles unique to, and largely conserved in, *S. cerevisiae* in the *COX1* gene that represent candidate determinants of the mitochondrial effects we study here (Figure S11). But we have also seen that phenotypic impacts differ among *S. cerevisiae* mitotypes, consistent with the extensive precedent for polymorphism among mitochondrial genomes and their effects on human disease (Wallace 2015) as well as traits in other animal models (Mossman et al. 2016 Nov 14; Mossman et al. 2016; Patel et al. 2016; Tsai and St. John 2016; Camus et al. 2017; Camus and Dowling 2018; Mossman et al. 2019; Camus et al. 2020; Salminen and Vale 2020; Anderson et al. 2022; Brand et al. 2024; Serrano et al. 2024) and plants (Dubrovina and Kiselev 2016; Adhikari et al. 2019; Jo et al. 2019). Furthermore, none of our mitochondrial manipulations reconstituted more than a fraction of the phenotype of the *S. cerevisiae* wild-type in the *S. paradoxus* background, congruent with the very modest effects of *S. cerevisiae* nuclear alleles known to be adaptive in this system (Weiss et al. 2018; AlZaben et al. 2021). Thus, our findings deepen the emerging picture of a highly complex architecture for yeast thermotolerance, with mitochondrial variants and many nuclear loci of small to modest effect coming together along the *S. cerevisiae* lineage to build the adaptation.

Our data also make clear that alongside largely beneficial marginal effects, all but one of the *S. cerevisiae* mitotypes we study are even more advantageous at high temperature in the context of pro-thermotolerance nuclear alleles (the exception being the mitotype from Dutch soil isolate

250 DBVPG1373). To date, such evidence for positive epistasis has been at a premium in the
251 literature describing adaptive loci from the wild (Nelson and Grishin 2018; Syenina et al. 2020;
252 Stern et al. 2022). This may be in part owing to a heavier emphasis in the field on negative
253 epistasis in the evolutionarily difficult repacking of a given protein interior to achieve fitness
254 (Weinreich et al. 2005; Starr and Thornton 2016), which could be more constrained than
255 combinations of adaptive alleles of multiple proteins. And negative epistasis has been rife
256 between mitochondrial and nuclear variants in analysis of traits that are not likely to promote
257 fitness, including reproductive barriers and aging and disease (Ellison and Burton 2008; Arnqvist
258 et al. 2010; Tranah 2011; Joseph et al. 2013; Lovell et al. 2015; Roux et al. 2016; Loewen and
259 Ganetzky 2018; Wolters et al. 2018; Sujkowski et al. 2019; Nguyen et al. 2020; Bushel et al.
260 2022; Biot-Pelletier et al. 2023; Nguyen et al. 2023; Ibrahim et al. 2024). But even in the
261 unlinked nuclear genes contributing to yeast thermotolerance, negative epistasis is the rule
262 rather than the exception (AlZaben et al. 2021). As such, our data point to pro-thermotolerance
263 mitoalleles as uniquely subject to positive epistasis with the nuclear genome in this adaptive
264 system. Under one compelling model, these mitochondrial variants may have been especially
265 easily accessible (Liao et al. 2022) and beneficial to populations during the evolution of *S.*
266 *cerevisiae* thermotolerance, representing the so-called low-hanging fruit (Lenski 2017) of the
267 adaptive process.

268 Though our data leave open the precise mechanism for such benefits, we propose that *S.*
269 *cerevisiae* mitotypes produce extra energy and metabolites (Malecki et al. 2020) during thermal
270 stress via enhanced respiration, relative to the putatively ancestral phenotypic program
271 attributable to mitochondria from *S. paradoxus*. If so, an excess of basic building blocks would
272 support the capacity of *S. cerevisiae* nuclear genes to confer their effects. The nuclear loci we
273 study here govern housekeeping functions, namely cell division and transcription/translation,
274 and some may prove to contribute more than others to the epistatic relationship with the
275 mitochondrial genome.

276 Meanwhile, the growth defects we have seen by cybrids at lower temperatures dovetail with
277 results from studies of *S. cerevisiae* nuclear thermotolerance loci and those using interspecies
278 backgrounds (Baker et al. 2019; Li et al. 2019; Hewitt et al. 2020; AlZaben et al. 2021). As a
279 general rule, evolutionary tradeoffs are routine in the adaptation literature, from prokaryotes
280 (Abram et al. 2021; Backman et al. 2024; Dalldorf et al. 2024) to animals (Ou et al. 2020;
281 Ackermans 2023; Metzler et al. 2023) and plants (Gao et al. 2022; He et al. 2022; Kurepa and
282 Smalle 2023). For yeast in particular, the exact mechanism of antagonistic pleiotropy exhibited
283 by thermotolerance loci in cooler conditions remains unclear. Exciting recent work has revealed
284 that *S. cerevisiae* proteins, including those encoded by mitochondria, are more thermostable
285 than those of sister species, establishing the likely biochemical underpinning of the trait
286 (Walunjkar et al. 2025). But it may not follow that the *S. cerevisiae* alleles of the loci we study
287 here compromise protein structure *per se* at low temperatures (Yang et al. 2015; Cui et al.
288 2024). Amino acid changes unique to *S. cerevisiae* could well have tuned the temperature
289 optima for the function of many enzymes, as appears to be the case for the thermotolerance
290 gene *DYN1* (Hong et al. 2016). Further work will be required to pinpoint exactly what
291 biochemical mechanisms *S. cerevisiae* gave up as it acquired pro-thermotolerance alleles. As
292 they stand, however, the genetics of this system help tell a story of a complex balancing act by
293 evolution along the *S. cerevisiae* lineage, as nuclear and mitochondrial variants were
294 assembled to convert a thermosensitive ancestor to a high-temperature specialist.

295 Materials and methods

296 **Strain construction**

297 Strains used in this study are listed in Table S1. For phenotyping in Figure S1, we used wild-
298 type, homozygous diploid *S. cerevisiae* strains DBVPG1373, YPS128, DBVPG6044 and Y55,
299 and *S. paradoxus* strains Z1, UFRJ50816, A4 and KPN3828, from the Saccharomyces Genome
300 Resequencing Project (SGRP) collection (Table S1) (Cubillos et al. 2009). To make haploid
301 strains for the recipients for *S. cerevisiae* mitochondrial DNA, we first generated prototrophic
302 versions of diploid *S. paradoxus* Z1 and the *S. paradoxus* harboring the eight *S. cerevisiae* loci,
303 designated as 8X (AlZaben et al. 2021). For this, the *HO* loci of the diploid wild-type Z1 and 8X
304 strains were knocked out using the hygromycin resistance gene as the selection marker using
305 the transformation protocol from (Reuß et al. 2004), with selection on 200 μg/ml hygromycin and
306 PCR and sequence confirmation. The resulting *ho*Δ::Hyg diploid strains were induced to
307 sporulate essentially as in (Lee et al. 2008), and mating types of the resulting haploids were
308 checked via halo assay following the protocol in (Hoffman et al. 2002), using JRY02375 and
309 JRY02176 as the mating testers. Next, for haploid MATα *S. paradoxus* Z1 and its descendant
310 8X, we generated a petite version of each (lacking mitochondrial DNA, ρ^0), using the protocol
311 adopted from (Amine et al. 2021). In short, yeast cells were streaked from -80°C stocks on
312 yeast peptone dextrose (YPD) plates and grown at 28°C for 2 days. A colony was inoculated
313 into 3 ml of YPD and incubated at 28°C overnight. 10^4 cells were inoculated into 1 ml of YPD
314 supplemented with ethidium bromide (EtBr, 10 μg/ml) and incubated at 28°C overnight. Cells
315 were harvested and washed twice with ddH_2O. About 200 cells were plated onto YPD plates
316 and grown at 28°C for 2-3 days to form visible colonies. The plates were replicated to yeast
317 peptone glycerol (YPG) plates to look for colonies that lost the ability to respire, *i.e.* those in the
318 ρ^0 state.

319 Finally, we used wild-type, MATα haploid, G418-resistant, hygromycin-resistant *S. cerevisiae*
320 strains DBVPG1373, YPS128, DBVPG6044, Y55 and DBVPG6765 from the SGRP collection
321 (Cubillos et al. 2009), and MATα haploid hygromycin-resistant *S. cerevisiae* strains (SJ6L01,
322 Sx3 and GE14S01-7B), a generous gift from Joseph Schacherer (Table S1) (Peter et al. 2018),
323 as donors of mitochondrial DNA for cybrids in *S. paradoxus* wild-type (Z1), 8X (Z1 with 8 *S.*
324 *cerevisiae* nuclear loci), and *S. cerevisiae* (DBVPG1373) backgrounds. Our method for cybrid
325 construction used the cytoduction protocol of (Nguyen et al. 2020) as follows. We first
326 constructed a heterokaryon-competent *S. cerevisiae* strain harboring each mitotype of interest,
327 referred to as a carrier. For this, a single colony of each donor in turn, and a single colony of the
328 ρ^0 *kar1*-d15 mutant (JRY5450, a generous gift from Dr. Jasper Rine), were each inoculated into
329 a separate 3 mL of liquid YPD (1% yeast extract, 2% peptone, 2% glucose) and incubated at
330 28°C overnight with shaking at 250 rpm. We mixed 100 μL of the two, spotted on a YPD plate,
331 and incubated at 28°C for 4 hours. The mixed cellular patch was inoculated into 3 mL of YPD
332 and incubated at 28°C for 2 hours with shaking at 250 rpm to promote cell division. After a 2-
333 hour incubation, 10^{-5} OD_{600} of cells were spread on a YPG plate (1% yeast extract, 2% peptone,
334 2% glycerol) to select for mitochondrial genome retention. Colonies on the YPG plates were
335 transferred to a YPD plate with 200 μg/mL hygromycin or 200 μg/mL G418 to check for
336 hygromycin and G418 sensitivity; we earmarked and preserved drug-sensitive, respiration-
337 competent strains as those in which the donor mitochondrial DNA had successfully been
338 transferred to the JRY5450 nuclear background. We next used each carrier strain in turn to
339 transfer the *S. cerevisiae* mitochondrial DNA of interest into the haploid *S. paradoxus* Z1 ρ^0
340 strain and, separately, its descendant, the 8X ρ^0 strain. This cytoduction proceeded as above
341 except that the carrier and the *S. paradoxus* strain were mated and the progeny were selected
342 on YPG alone; afterward we subjected them to the halo assay, to eliminate the carrier-*S.*
343 *paradoxus* diploid hybrids, and only those strains that behaved as haploid MATα were retained
344 as cybrids.

345 **Growth assays**

346 Measurements of cell density were done as described (AlZaben et al. 2021) with some
347 modifications. To make sure the cells were respiratory-competent before the assay, strains were
348 streaked on YPG plates and were allowed to grow at 28°C for 4 days to form colonies. Three
349 colonies were inoculated into 15 mL of liquid YPG and incubated at 28°C for overnight with
350 shaking at 250 rpm. The cultures reached 0.4-0.8 OD_{600} after a 16-hour growth; in these pre-
351 cultures, assays of glycogen and trehalose storage (see below) detected no difference between
352 genotypes (Figure S10). The cultures were then back-diluted into 5 mL of YPD, YPE (1% yeast
353 extract, 2% peptone, 2% ethanol), or YPG to achieve 0.1 OD_{600}/mL, and then incubated at
354 23°C, 28°C or 39°C for 24 hours. This procedure, from streaking on solid agar plates to biomass
355 measurement, was repeated at least twice for each strain with three technical repeats in each
356 biological replicate. We collected the readouts of cell density from all the replicates across all
357 days for a given strain and compared each mitochondrial transgenic to *S. paradoxus* with a two-
358 tailed Mann-Whitney U test. For epistasis analysis, a two-way ANOVA test was carried out to
359 examine the impact of the genotype-mitotype interaction on thermotolerance. All statistical
360 analyses were done with scipy.stats in Python 3.7.

361 **MTT assay**

362 To measure respiration efficiency, pre-culture and treatment were as in Growth assays, above,
363 and after 24 hours we carried out the MTT assay as in (Sánchez and Königsberg 2006).
364 Independent experiments from growth to MTT measurement were performed at least six times.
365 The readouts were normalized to that of wild-type *S. paradoxus* at either 28°C or 39°C. Two-
366 tailed one-sample Wilcoxon test was performed using the normalized data with a hypothesized
367 value of 1 with scipy.stats in Python 3.7.

368 **Growth of *S. cerevisiae* and *S. paradoxus* in glycerol**

369 Data are from (Liti et al. 2009) and Mann-Whitney U test was performed to compare the growths
370 of the two species in glycerol with scipy.stats in Python 3.7.

371 **Trehalose and glycogen assays**

372 To measure the contents of trehalose and glycogen stored in yeast, we took advantage of the
373 protocol from (Chen and Futcher 2017). Briefly, yeast cells were pre-grown in YPG overnight.
374 0.3 OD_{600} of cells were harvested, and the pellets were washed with 1 ml of ddH_2O to remove
375 residual media. The pellets were resuspended in 125 μl of 0.25 M Na_2CO_3 solution, and
376 incubated at 95°C for 3 hours in PCR tubes. 75 μl of 1 M acetic acid and 300 μl of 0.2 M sodium
377 acetate, pH 5.2 were added to the mix. The mix was immediately divided into two 250-μl
378 aliquots. For glycogen measurements, 10 μl of *Aspergillus niger* α-amyloglucosidase (20 mg/ml
379 in 0.2 M sodium acetate, pH 5.2) was added to one of the aliquots, and incubated at 57°C
380 overnight. For trehalose measurements, 15 μl of 0.2 M sodium acetate, pH 8 was added to the
381 other aliquot to adjust the pH to ~5.8, and then 3 μl of porcine trehalase was added to the
382 sample, and incubated at 37°C overnight. After overnight incubation, the content of glucose,
383 digested from either trehalose or glycogen, in each sample was measured using Glucose (GO)
384 Assay Kit (Cat. No. GAGO20) at absorbance of 540nm. OD_{540} readouts in this setting represent
385 the content of glucose in each sample, reporting the concentration of the substrates, trehalose
386 and glycogen, are in the cells.

387 **Multiple sequence alignment**

388 *S. cerevisiae* mitochondrial genomes were from (De Chiara et al. 2020). North American *S.*
389 *paradoxus* mitochondrial genomes (NCBI accessions: KY287641-KY287662) were from
390 (Leducq et al. 2017), and European and Asian *S. paradoxus* genomes (NCBI accessions:

391 JQ862335.1, KP712799.1, KP712802.1, KP712786.1, KP712796.1) were from (Procházka et al.
392 2012). Multiple sequence alignment was performed using Muscle v. 5.1. (Edgar 2022), the allele
393 frequency was calculated and plotted with Python 3.7, and the alignment was visualized with
394 AliView v. 3.0 (Larsson 2014).

395

396 # Figure captions

397 **Figure 1. Experimental design and isolates for genetic dissection of *Saccharomyces***
398 **species variation in thermotolerance.** Top, wild-type *S. paradoxus* (left) is used as the
399 background for a cybrid (right) harboring the endogenous nuclear genome (N) and the
400 mitochondrial genome from a *S. cerevisiae* donor (orange). Bottom, strains used in this work:
401 Sp, *S. paradoxus* Z1; Sc1 to Sc8, *S. cerevisiae* DBVPG1373, YPS128, DBVPG6044, Y55,
402 SJ6L01, SX3, GE14S01-7B, and DBVPG6765, respectively.

403 **Figure 2. Condition-dependent growth and tradeoffs across cybrids. (A)** Each cell reports
404 cell density, as a mean across replicates ($n \geq 3$), after 24 hours of growth in liquid culture in the
405 respective condition, with glucose as the carbon source unless otherwise indicated. Each
406 column reports results from wild-type *S. paradoxus* (Sp) or an isogenic cybrid harboring the
407 mitochondrial genome from a *S. cerevisiae* donor (Scmt) labeled as in Figure 1. Colors report
408 row-normalized z-score. **(B-D)** Shown are reanalyses of cell density measurements across
409 strains from the cultures and conditions in **(A)**, with respective Spearman coefficients of -0.8, 1,
410 and 0.67. In a given panel, each dot reports median across replicates ($n \geq 3$), and error bars
411 report standard deviation. Strain labels are as in **(A)**. *, Growth different from that of *S.*
412 *paradoxus* at two-tailed Mann-Whitney $p < 0.05$. Raw growth measurements, Spearman
413 correlation coefficients, and statistical analyses are reported in Table S2A to G.

414 **Figure 3. *S. cerevisiae* mitotypes boost respiration in the *S. paradoxus* nuclear**
415 **background at 39°C.** In each panel, in the main plot, the *y*-axis reports measurements of the
416 reduction of 1-(4,5-dimethylthiazol-2-yl)-3,5-diphenyltetrazolium bromide after 24 hours of
417 growth of a given strain in liquid culture with glucose as the carbon source at one temperature,
418 normalized to the respective measurement wild-type *S. paradoxus*. In a given column, each
419 point reports results from one biological replicate and the bar height reports the average. The *x*-
420 axis denotes strain genotypes: wild-type *S. paradoxus* (Sp) or cybrids each harboring the
421 mitochondrial genome from a *S. cerevisiae* donor (Scmt) labeled as in Figure 1. **(A),** 28°C; **(B)**,
422 39°C. *, one-sample Wilcoxon $p < 0.05$. Raw data and statistical analyses are reported in Table
423 S2H and I.

424 **Figure 4. Epistasis between nuclear and mitochondrial *Saccharomyces* species variants**
425 **that impact thermotolerance.** In a given column, each color reports results from 24 hours of
426 growth at 39°C, with glucose as the carbon source, of a strain of *S. paradoxus* with (8X) or
427 without (WT) 8 thermotolerance loci from *S. cerevisiae*, harboring an *S. cerevisiae* mitotype.
428 The *y*-axis reports the cell density of the indicated strain normalized to that of *S. paradoxus* with
429 its native mitotype. Strain genotypes are as in Figure 1. Each point reports one replicate ($n \geq 6$).
430 *, the interaction term from a two-factor ANOVA with mitotype and nuclear genotype as factors
431 was significant at $p < 0.01$. Raw growth measurements and statistical analyses are reported in
432 Table S2A and J.

433

434

435

436 Supplementary figure captions

437 **Figure S1. Stark growth differences between *S. cerevisiae* and *S. paradoxus* at high**
438 **temperature.** In a given panel, the *y*-axis reports cell density after 24 hours of growth in liquid
439 culture of a wild-type homozygous diploid *Saccharomyces* strain in one temperature condition,
440 with glucose as the carbon source. Points reports technical replicates (n = 3) and bar heights
441 report means. Sc1, Sc2, Sc3 and Sc4 denote *S. cerevisiae* DBVPG1373, YPS128, DBVPG6044
442 and Y55, respectively. Sp1, Sp2, Sp3 and Sp4 denote *S. paradoxus* KPN3828, UFRJ50816, A4
443 and Z1, respectively. **(A)** 28°C; **(B)** 39°C. *, two-tailed Mann-Whitney $p < 0.05$. Raw growth
444 measurements and statistical analyses are reported in Table S2K.

445 **Figure S2. Wild-type strain and species variation in growth on glycerol.** In a given panel,
446 each bar reports results from the indicated wild-type *S. cerevisiae* or *S. paradoxus* strain grown
447 in liquid culture with glycerol as the carbon source, normalized with respect to a standard
448 reference-strain control, from (Warringer et al. 2011). The *y*-axis reports relative growth rate **(A)**
449 and efficiency **(B)**. *, two-tailed Mann-Whitney $p < 0.05$. Raw growth measurements and
450 statistical analyses are reported in Table S2L to S2N.

451 **Figure S3. Condition-dependent growth across *Saccharomyces* species and cybrids.**
452 Data are as in Figure 2A except that wild-type *S. cerevisiae* (DBVPG1373) is included. Raw
453 growth measurements and statistical analyses are reported in Table S2A to S2G.

454 **Figure S4. *S. cerevisiae* mitotypes boost respiration in the *S. paradoxus* nuclear**
455 **background at 39°C with addition of *S. cerevisiae*.** Data are as in Figure 3 except that wild-
456 type *S. cerevisiae* (DBVPG1373) is included. Raw MTT measurements and statistical analyses
457 are reported in Table S2H and S2I.

458 **Figure S5. *S. cerevisiae* mitotypes are sufficient to boost thermotolerance in *S.***
459 ***paradoxus*.** Each column reports results from *S. paradoxus* harboring mitochondrial DNA from
460 a *S. cerevisiae* strain. The *y*-axis reports cell density after 24 hours of growth at 39°C of a cybrid
461 normalized to that of the wild-type *S. paradoxus*, which is shown as the dashed line. *, two-
462 tailed Mann-Whitney $p < 0.05$. Bar height reports average across replicates, and each dot is one
463 technical or biological replicate. Scmt 1 to Scmt 8 denote mitotypes from Sc 1 to Sc 8 in Figure
464 1. Raw growth measurements and statistical analyses are reported in Table S2A and S2O.

465 **Figure S6. Effects of *S. cerevisiae* mitotypes in *S. cerevisiae* on thermotolerance echo**
466 **those in *S. paradoxus*.** Each column reports results from *S. cerevisiae* harboring mitochondrial
467 DNA from a *S. cerevisiae* strain. The *y*-axis reports cell density after 24 hours of growth at 39°C.
468 *, two-tailed Mann-Whitney $p < 0.05$. Bar height reports average across replicates, and each dot
469 is one technical or biological replicate. Labels on the *x*-axis are as in Figure 2A. Raw growth
470 measurements and statistical analyses are reported in Table S2A and S2J.

471 **Figure S7. Chronic 39°C treatment is lethal to *S. paradoxus* and its cybrids.** Shown are
472 results of plating of the indicated strains after 24 hours of culture in one temperature condition,
473 with glucose as the carbon source, followed by incubation of plates at 28°C for two days. Strains
474 were wild-type *S. cerevisiae* (Sc), wild-type *S. paradoxus* (Sp), or a cybrid in the *S. paradoxus*
475 background harboring the mitochondrial genome from a *S. cerevisiae* donor (Scmt) labeled as
476 in Figure 1 of the main text.

477 **Figure S8. Chronic 39°C treatment is lethal to *S. paradoxus* harboring *S. cerevisiae***
478 **nuclear thermotolerance loci and to its cybrids.** Labels are as in Figure S7 except that the
479 strains were wild-type *S. cerevisiae* (Sc), wild-type *S. paradoxus* (Sp), *S. paradoxus* harboring

480 eight nuclear loci from *S. cerevisiae* (8X), or a cybrid in the 8X background harboring the
481 mitochondrial genome from a *S. cerevisiae* donor (Scmt) labeled as in Figure 1 of the main text.

482 **Figure S9. No detectable epistasis between nuclear and mitochondrial *Saccharomyces***
483 **species variants that impact 28°C growth.** Data are as Figure 4 of the main text except that
484 cell densities were measured after 24 hours of growth at 28°C. Raw growth measurements and
485 statistical analyses are reported in Table S2A and S2J.

486 **Figure S10. No detectable differences in glycogen and trehalose storage in *S. paradoxus***
487 **cybrids.** In a given panel, each bar reports energy storage by cells of the indicated strain after
488 growth with glycerol as the carbon source at 28°C, either glycogen (A) or trehalose (B). Each
489 dot denotes one biological or technical replicate. Labels on the *x*-axis are as in Figure 2A of the
490 main text. Raw trehalose and glycogen measurements and statistical analyses are reported in
491 Table S2P and S2Q.

492 **Figure S11. A multiple sequence alignment analysis shows highly diverged amino acid**
493 **variants in *COX1* between *S. paradoxus* and *S. cerevisiae*.** At top, each line reports one
494 *COX1* amino acid sequence of *S. cerevisiae* (737 strains) and *S. paradoxus* (27 strains) as
495 denoted on the left. At bottom, bar heights in each panel report the frequency of the indicated
496 amino acid allele in the indicated species. Not shown are infrequent alleles in *S. cerevisiae*.,
497 namely N (0.3%) and T (0.1%) at position 55 and premature stop codons (0.3%) at position 58.
498 Mitochondrial genome accessions are cited in the Materials and Methods section.

499

500 Supplementary table captions

501 **Table S1. Strains used in this work.**

502 **Table S2. Growth data and statistics.** D1373, YPS128, D6044 and Y55 indicate *S. cerevisiae*
503 strains DBVPG1373, YPS128, DBVPG6044 and Y55, respectively; Sp, *S. paradoxus* Z1. Table
504 S2A contains all OD_{600} measurements of each strain at 39°C in standard glucose medium. Table
505 S2B reports the statistical analysis of the OD_{600} measurements of the cybrids in **(A)** compared to
506 wild-type *S. paradoxus* or the *S. paradoxus* harboring *S. cerevisiae* nuclear loci (8X) by Mann-
507 Whitney U test. Table S2C contains all OD_{600} measurements of each strain at 28°C in standard
508 glucose medium. Table S2D contains all OD_{600} measurements of each strain at 28°C in medium
509 with glycerol as a carbon source. Table S2E contains all OD_{600} measurements of each strain at
510 28°C in medium with ethanol as a carbon source. Table S2F contains all OD_{600} measurements
511 of each strain at 23°C in standard glucose medium. Table S2G reports the Spearman correlation
512 coefficients and respective *p*-values of Figures 2B, 2C and 2D. Table 2H reports the raw
513 readouts of the MTT assay at 28°C and 39°C. Table 2I reports the *p*-values of the normalized
514 MTT measurements by one-sample Wilcoxon with a hypothesized value of 1. Tabel S2J reports
515 the *p*-values of two-way ANOVA of the impact of the interaction between *S. cerevisiae* mitotypes
516 and the 8 *S. cerevisiae* loci in the *S. paradoxus* background on high temperature growth (Figure
517 4). Table S2K reports reports the OD_{600} measurements of wild-type *S. cerevisiae* and *S.*
518 *paradoxus* strains at 28°C and 39°C in standard glucose medium with the statistical analysis
519 (Figure S1). Table S2L and S2M report the growth efficiency and rate in glycerol as the carbon
520 source from (Warringer et al. 2011). Table S2N reports the *p*-values of glycerol growth efficiency
521 and rate of the wild-type *S. cerevisiae* and *S. paradoxus* strains by two-tailed Mann-Whitney U
522 test (Warringer et al. 2011) (Figure S2). Table S2O reports the *p*-values of Figure S5 by two-
523 tailed Mann-Whitney U test. Table S2P and S2Q report the raw readouts of trehalose and
524 glycogen assays and *p*-values by two-tailed Mann-Whitney U test, respectively (Figure S10).

525

References

Abram F, Arcari T, Guerreiro D, O'Byrne CP. 2021. Evolutionary trade-offs between growth and survival: The delicate balance between reproductive success and longevity in bacteria. In: Advances in Microbial Physiology. Vol. 79. Elsevier; p 133–162 https://linkinghub.elsevier.com/retrieve/pii/S006529112100014X. https://doi.org/10.1016/bs.ampbs.2021.07.002

Abrams MB et al. 2021. Population and comparative genetics of thermotolerance divergence between yeast species Gresham D, editor. G3. 11(7):jkab139. https://doi.org/10.1093/g3journal/jkab139

Ackermans NL. 2023. Neurobiological tradeoffs of headbutting bovids. Trends in Neurosciences. 46(11):898–900. https://doi.org/10.1016/j.tins.2023.08.004

Adhikari B, Caruso CM, Case AL. 2019. Beyond balancing selection: frequent mitochondrial recombination contributes to high-female frequencies in gynodioecious *Lobelia siphilitica* (Campanulaceae). New Phytologist. 224(3):1381–1393. https://doi.org/10.1111/nph.16136

Allen Orr H. 2001. The genetics of species differences. Trends in Ecology & Evolution. 16(7):343–350. https://doi.org/10.1016/S0169-5347(01)02167-X

AlZaben F, Chuong JN, Abrams MB, Brem RB. 2021. Joint effects of genes underlying a temperature specialization tradeoff in yeast Fay JC, editor. PLoS Genet. 17(9):e1009793. https://doi.org/10.1371/journal.pgen.1009793

Amine AAA et al. 2021. Experimental evolution improves mitochondrial genome quality control in Saccharomyces cerevisiae and extends its replicative lifespan. Current Biology. 31(16):3663-3670.e4. https://doi.org/10.1016/j.cub.2021.06.026

Anderson L et al. 2022. Variation in mitochondrial DNA affects locomotor activity and sleep in Drosophila melanogaster. Heredity. 129(4):225–232. https://doi.org/10.1038/s41437-022-00554-w

Arnqvist G et al. 2010. Genetic architecture of metabolic rate: environment specific epistasis between mitochondrial and nuclear genes in an insect. Evolution. 64(12):3354–3363. https://doi.org/10.1111/j.1558-5646.2010.01135.x

Backman T, Burbano HA, Karasov TL. 2024. Tradeoffs and constraints on the evolution of tailocins. Trends in Microbiology. 32(11):1084–1095. https://doi.org/10.1016/j.tim.2024.04.001

Baker EP et al. 2019. Mitochondrial DNA and temperature tolerance in lager yeasts. Sci Adv. 5(1):eaav1869. https://doi.org/10.1126/sciadv.aav1869

Bazzicalupo A. 2022. Local adaptation in fungi. FEMS Microbiology Reviews. 46(6):fuac026. https://doi.org/10.1093/femsre/fuac026

Biot-Pelletier D et al. 2023. Evolutionary Trajectories are Contingent on Mitonuclear Interactions Zhang J, editor. Molecular Biology and Evolution. 40(4):msad061. https://doi.org/10.1093/molbev/msad061

563 Bozdag GO et al. 2021. Breaking a species barrier by enabling hybrid recombination. Current
564 Biology. 31(4):R180–R181. https://doi.org/10.1016/j.cub.2020.12.038

565 Brand JA, Garcia-Gonzalez F, Dowling DK, Wong BBM. 2024. Mitochondrial genetic variation as
566 a potential mediator of intraspecific behavioural diversity. Trends in Ecology & Evolution.
567 39(2):199–212. https://doi.org/10.1016/j.tree.2023.09.009

568 Bushel PR et al. 2022. Mitochondrial-nuclear epistasis underlying phenotypic variation in breast
569 cancer pathology. Sci Rep. 12(1):1393. https://doi.org/10.1038/s41598-022-05148-4

570 Camus MF, Dowling DK. 2018. Mitochondrial genetic effects on reproductive success:
571 signatures of positive intrasexual, but negative intersexual pleiotropy. Proc Biol Sci.
572 285(1879):20180187. https://doi.org/10.1098/rspb.2018.0187

573 Camus MF, O'Leary M, Reuter M, Lane N. 2020. Impact of mitonuclear interactions on life-
574 history responses to diet. Phil Trans R Soc B. 375(1790):20190416.
575 https://doi.org/10.1098/rstb.2019.0416

576 Camus MF, Wolff JN, Sgrò CM, Dowling DK. 2017. Experimental Support That Natural Selection
577 Has Shaped the Latitudinal Distribution of Mitochondrial Haplotypes in Australian Drosophila
578 melanogaster. Mol Biol Evol. 34(10):2600–2612. https://doi.org/10.1093/molbev/msx184

579 Cao Y et al. 2022. Sex differences in heart mitochondria regulate diastolic dysfunction. Nat
580 Commun. 13(1):3850. https://doi.org/10.1038/s41467-022-31544-5

581 Chen Y, Futcher B. 2017. Assaying Glycogen and Trehalose in Yeast. Bio Protoc. 7(13):e2371.
582 https://doi.org/10.21769/BioProtoc.2371

583 Chou J-Y et al. 2010. Multiple Molecular Mechanisms Cause Reproductive Isolation between
584 Three Yeast Species Noor MAF, editor. PLoS Biol. 8(7):e1000432.
585 https://doi.org/10.1371/journal.pbio.1000432

586 Chou J-Y, Leu J-Y. 2015. The Red Queen in mitochondria: cyto-nuclear co-evolution, hybrid
587 breakdown and human disease. Front Genet. 6 [accessed 2025 Feb 18].
588 http://www.frontiersin.org/Evolutionary_and_Population_Genetics/10.3389/fgene.2015.00187/ab
589 stract. https://doi.org/10.3389/fgene.2015.00187

590 Crandall JG, Fisher KJ, Sato TK, Hittinger CT. 2023. Ploidy evolution in a wild yeast is linked to
591 an interaction between cell type and metabolism Zanders SE, editor. PLoS Biol.
592 21(11):e3001909. https://doi.org/10.1371/journal.pbio.3001909

593 Cubillos FA, Louis EJ, Liti G. 2009. Generation of a large set of genetically tractable haploid and
594 diploid *Saccharomyces* strains. FEMS Yeast Research. 9(8):1217–1225.
595 https://doi.org/10.1111/j.1567-1364.2009.00583.x

596 Cui S, Furukawa R, Akanuma S. 2024. Insights into the low-temperature adaptation of an
597 enzyme as studied through ancestral sequence reconstruction. [accessed 2024 Dec 16].
598 http://biorxiv.org/lookup/doi/10.1101/2024.09.05.611558.
599 https://doi.org/10.1101/2024.09.05.611558

600 Dalldorf C et al. 2024. The hallmarks of a tradeoff in transcriptomes that balances stress and
601 growth functions Fodor A, editor. mSystems. 9(7):e00305-24.
602 https://doi.org/10.1128/msystems.00305-24

603 De Chiara M et al. 2020. Discordant evolution of mitochondrial and nuclear yeast genomes at
604 population level. BMC Biol. 18(1):49. https://doi.org/10.1186/s12915-020-00786-4

605 Dubrovina AS, Kiselev KV. 2016. Age-associated alterations in the somatic mutation and DNA
606 methylation levels in plants Weber A, editor. Plant Biol J. 18(2):185–196.
607 https://doi.org/10.1111/plb.12375

608 Edgar RC. 2022. Muscle5: High-accuracy alignment ensembles enable unbiased assessments
609 of sequence homology and phylogeny. Nat Commun. 13(1):6968.
610 https://doi.org/10.1038/s41467-022-34630-w

611 Elena SF. 2017. Local adaptation of plant viruses: lessons from experimental evolution.
612 Molecular Ecology. 26(7):1711–1719. https://doi.org/10.1111/mec.13836

613 Ellison CK, Burton RS. 2008. Genotype-dependent variation of mitochondrial transcriptional
614 profiles in interpopulation hybrids. Proc Natl Acad Sci USA. 105(41):15831–15836.
615 https://doi.org/10.1073/pnas.0804253105

616 Ferreira T, Rodriguez S. 2024. Mitochondrial DNA: Inherent Complexities Relevant to Genetic
617 Analyses. Genes. 15(5):617. https://doi.org/10.3390/genes15050617

618 Forejt J, Jansa P. 2023. Meiotic Recognition of Evolutionarily Diverged Homologs:
619 Chromosomal Hybrid Sterility Revisited Malik H, editor. Molecular Biology and Evolution.
620 40(4):msad083. https://doi.org/10.1093/molbev/msad083

621 Fredericks LR et al. 2021. The Species-Specific Acquisition and Diversification of a K1-like
622 Family of Killer Toxins in Budding Yeasts of the Saccharomycotina. PLoS Genet.
623 17(2):e1009341. https://doi.org/10.1371/journal.pgen.1009341

624 Gao H et al. 2022. Natural variations of ZmSRO1d modulate the trade-off between drought
625 resistance and yield by affecting ZmRBOHC-mediated stomatal ROS production in maize.
626 Molecular Plant. 15(10):1558–1574. https://doi.org/10.1016/j.molp.2022.08.009

627 Gonçalves P et al. 2011. Evidence for Divergent Evolution of Growth Temperature Preference in
628 Sympatric Saccharomyces Species Chaturvedi V, editor. PLoS ONE. 6(6):e20739.
629 https://doi.org/10.1371/journal.pone.0020739

630 He Z, Webster S, He SY. 2022. Growth–defense trade-offs in plants. Current Biology.
631 32(12):R634–R639. https://doi.org/10.1016/j.cub.2022.04.070

632 Hénault M, Marsit S, Charron G, Landry CR. 2022. Hybridization drives mitochondrial DNA
633 degeneration and metabolic shift in a species with biparental mitochondrial inheritance. Genome
634 Res. 32(11–12):2043–2056. https://doi.org/10.1101/gr.276885.122

635 Hewitt SK et al. 2020. Plasticity of Mitochondrial DNA Inheritance and its Impact on Nuclear
636 Gene Transcription in Yeast Hybrids. Microorganisms. 8(4):494.
637 https://doi.org/10.3390/microorganisms8040494

638 Hoffman GA, Garrison TR, Dohlman HG. 2002. Analysis of RGS Proteins in Saccharomyces
639 cerevisiae. In: Methods in Enzymology. Vol. 344. Elsevier; p 617–631 [accessed 2024 Dec 17].
640 https://linkinghub.elsevier.com/retrieve/pii/S0076687902447441. https://doi.org/10.1016/S0076-
641 6879(02)44744-1

642 Hong W et al. 2016. The Effect of Temperature on Microtubule-Based Transport by Cytoplasmic
643 Dynein and Kinesin-1 Motors. Biophysical Journal. 111(6):1287–1294.
644 https://doi.org/10.1016/j.bpj.2016.08.006

645 Hou J, Friedrich A, de Montigny J, Schacherer J. 2014. Chromosomal Rearrangements as a
646 Major Mechanism in the Onset of Reproductive Isolation in Saccharomyces cerevisiae. Current
647 Biology. 24(10):1153–1159. https://doi.org/10.1016/j.cub.2014.03.063

648 Houtkooper RH et al. 2013. Mitonuclear protein imbalance as a conserved longevity
649 mechanism. Nature. 497(7450):451–457. https://doi.org/10.1038/nature12188

650 Ibrahim R, Bahilo Martinez M, Dobson AJ. 2024. Rapamycin's lifespan effect is modulated by
651 mito-nuclear epistasis in *Drosophila*. Aging Cell. e14328. https://doi.org/10.1111/acel.14328

652 Jain AK et al. 2018. Models and Methods for In Vitro Toxicity. In: In Vitro Toxicology. Elsevier; p
653 45–65 [accessed 2025 Feb 25].
654 https://linkinghub.elsevier.com/retrieve/pii/B9780128046678000031.
655 https://doi.org/10.1016/B978-0-12-804667-8.00003-1

656 Jhuang H, Lee H, Leu J. 2017. Mitochondrial–nuclear co-evolution leads to hybrid
657 incompatibility through pentatricopeptide repeat proteins. EMBO Reports. 18(1):87–101.
658 https://doi.org/10.15252/embr.201643311

659 Jo YD et al. 2019. Mitotypes Based on Structural Variation of Mitochondrial Genomes Imply
660 Relationships With Morphological Phenotypes and Cytoplasmic Male Sterility in Peppers. Front
661 Plant Sci. 10:1343. https://doi.org/10.3389/fpls.2019.01343

662 Joseph B et al. 2013. Cytoplasmic genetic variation and extensive cytonuclear interactions
663 influence natural variation in the metabolome. eLife. 2:e00776.
664 https://doi.org/10.7554/eLife.00776

665 Kellis M et al. 2003. Sequencing and comparison of yeast species to identify genes and
666 regulatory elements. Nature. 423(6937):241–254. https://doi.org/10.1038/nature01644

667 Kraemer SA, Boynton PJ. 2017. Evidence for microbial local adaptation in nature. Molecular
668 Ecology. 26(7):1860–1876. https://doi.org/10.1111/mec.13958

669 Kurepa J, Smalle JA. 2023. Plant Hormone Modularity and the Survival-Reproduction Trade-Off.
670 Biology. 12(8):1143. https://doi.org/10.3390/biology12081143

671 Larsson A. 2014. AliView: a fast and lightweight alignment viewer and editor for large datasets.
672 Bioinformatics. 30(22):3276–3278. https://doi.org/10.1093/bioinformatics/btu531

673 Leducq J-B et al. 2017. Mitochondrial Recombination and Introgression during Speciation by
674 Hybridization. Molecular Biology and Evolution. 34(8):1947–1959.
675 https://doi.org/10.1093/molbev/msx139

676 Lee H-Y et al. 2008. Incompatibility of Nuclear and Mitochondrial Genomes Causes Hybrid
677 Sterility between Two Yeast Species. Cell. 135(6):1065–1073.
678 https://doi.org/10.1016/j.cell.2008.10.047

679 Lenski RE. 2017. Experimental evolution and the dynamics of adaptation and genome evolution
680 in microbial populations. The ISME Journal. 11(10):2181–2194.
681 https://doi.org/10.1038/ismej.2017.69

682 Li XC et al. 2019. Mitochondria-encoded genes contribute to evolution of heat and cold
683 tolerance in yeast. Sci Adv. 5(1):eaav1848. https://doi.org/10.1126/sciadv.aav1848

684 Liao S, Chen L, Song Z, He H. 2022. The fate of damaged mitochondrial DNA in the cell.
685 Biochimica et Biophysica Acta (BBA) - Molecular Cell Research. 1869(5):119233.
686 https://doi.org/10.1016/j.bbamcr.2022.119233

687 Liti G et al. 2009. Population genomics of domestic and wild yeasts. Nature. 458(7236):337–
688 341. https://doi.org/10.1038/nature07743

689 Loewen CA, Ganetzky B. 2018. Mito-Nuclear Interactions Affecting Lifespan and
690 Neurodegeneration in a *Drosophila* Model of Leigh Syndrome. Genetics. 208(4):1535–1552.
691 https://doi.org/10.1534/genetics.118.300818

692 Lovell JT et al. 2015. Exploiting Differential Gene Expression and Epistasis to Discover
693 Candidate Genes for Drought-Associated QTLs in *Arabidopsis thaliana*. Plant Cell. 27(4):969–
694 983. https://doi.org/10.1105/tpc.15.00122

695 Lupo O, Krieger G, Jonas F, Barkai N. 2021. Accumulation of *cis* - and *trans* -regulatory
696 variations is associated with phenotypic divergence of a complex trait between yeast species
697 Andrews B, editor. G3 Genes|Genomes|Genetics. 11(2):jkab016.
698 https://doi.org/10.1093/g3journal/jkab016

699 Malecki M, Kamrad S, Ralser M, Bähler J. 2020. Mitochondrial respiration is required to provide
700 amino acids during fermentative proliferation of fission yeast. EMBO Reports. 21(11):e50845.
701 https://doi.org/10.15252/embr.202050845

702 Mário Š, Poláková S, Jatzová K, Sulo P. 2015. Post-zygotic sterility and cytonuclear
703 compatibility limits in S. cerevisiae xenomitochondrial cybrids. Front Genet. 5 [accessed 2024
704 Nov 7]. http://journal.frontiersin.org/article/10.3389/fgene.2014.00454/abstract.
705 https://doi.org/10.3389/fgene.2014.00454

706 Marsit S et al. 2021. The neutral rate of whole-genome duplication varies among yeast species
707 and their hybrids. Nat Commun. 12(1):3126. https://doi.org/10.1038/s41467-021-23231-8

708 Melvin RG, Ballard JWO. 2006. Intraspecific variation in survival and mitochondrial oxidative
709 phosphorylation in wild-caught *Drosophila simulans*. Aging Cell. 5(3):225–233.
710 https://doi.org/10.1111/j.1474-9726.2006.00211.x

711 Meng X et al. 2022. GWAS on multiple traits identifies mitochondrial ACONITASE3 as important
712 for acclimation to submergence stress. Plant Physiology. 188(4):2039–2058.
713 https://doi.org/10.1093/plphys/kiac011

714 Metzler S, Kirchner J, Grasse AV, Cremer S. 2023. Trade-offs between immunity and
715 competitive ability in fighting ant males. BMC Ecol Evo. 23(1):37.
716 https://doi.org/10.1186/s12862-023-02137-7

717 Moran BM et al. 2024. A lethal mitonuclear incompatibility in complex I of natural hybrids.
718 Nature. 626(7997):119–127. https://doi.org/10.1038/s41586-023-06895-8

719 Mossman JA et al. 2016. Mitonuclear Interactions Mediate Transcriptional Responses to
720 Hypoxia in *Drosophila*. Mol Biol Evol. msw246. https://doi.org/10.1093/molbev/msw246

721 Mossman JA, Biancani LM, Rand DM. 2019. Mitochondrial genomic variation drives differential
722 nuclear gene expression in discrete regions of Drosophila gene and protein interaction
723 networks. BMC Genomics. 20(1):691. https://doi.org/10.1186/s12864-019-6061-y

724 Mossman JA, Biancani LM, Zhu C-T, Rand DM. 2016. Mitonuclear Epistasis for Development
725 Time and Its Modification by Diet in *Drosophila*. Genetics. 203(1):463–484.
726 https://doi.org/10.1534/genetics.116.187286

727 Nelson ED, Grishin NV. 2018. Inference of epistatic effects in a key mitochondrial protein. Phys
728 Rev E. 97(6):062404. https://doi.org/10.1103/PhysRevE.97.062404

729 Nguyen THM et al. 2020. Mitochondrial-nuclear coadaptation revealed through mtDNA
730 replacements in Saccharomyces cerevisiae. BMC Evol Biol. 20(1):128.
731 https://doi.org/10.1186/s12862-020-01685-6

732 Nguyen THM et al. 2023. Mapping mitonuclear epistasis using a novel recombinant yeast
733 population Hopper AK, editor. PLoS Genet. 19(3):e1010401.
734 https://doi.org/10.1371/journal.pgen.1010401

735 Nikolov LA, Tsiantis M. 2015. Interspecies Gene Transfer as a Method for Understanding the
736 Genetic Basis for Evolutionary Change: Progress, Pitfalls, and Prospects. Front Plant Sci.
737 6:1135. https://doi.org/10.3389/fpls.2015.01135

738 Oppong RF et al. 2022. Personality traits are consistently associated with blood mitochondrial
739 DNA copy number estimated from genome sequences in two genetic cohort studies. eLife.
740 11:e77806. https://doi.org/10.7554/eLife.77806

741 Ou Q et al. 2020. Evolutionary trade-off in reproduction of Cambrian arthropods. Sci Adv.
742 6(18):eaaz3376. https://doi.org/10.1126/sciadv.aaz3376

743 Paget CM, Schwartz J-M, Delneri D. 2014. Environmental systems biology of cold-tolerant
744 phenotype in Saccharomyces species adapted to grow at different temperatures. Mol Ecol.
745 23(21):5241–5257. https://doi.org/10.1111/mec.12930

746 Pakendorf B, Stoneking M. 2005. MITOCHONDRIAL DNA AND HUMAN EVOLUTION. Annu
747 Rev Genom Hum Genet. 6(1):165–183.
748 https://doi.org/10.1146/annurev.genom.6.080604.162249

749 Parra M et al. 2023. Assembly and comparative genome analysis of a Patagonian
750 *Aureobasidium pullulans* isolate reveals unexpected intraspecific variation. Yeast. 40(5–6):197–
751 213. https://doi.org/10.1002/yea.3853

752 Patel MR et al. 2016. A mitochondrial DNA hypomorph of cytochrome oxidase specifically
753 impairs male fertility in Drosophila melanogaster. eLife. 5:e16923.
754 https://doi.org/10.7554/eLife.16923

755 Peng L, Wang B, Ren P. 2005. Reduction of MTT by flavonoids in the absence of cells. Colloids
756 and Surfaces B: Biointerfaces. 45(2):108–111. https://doi.org/10.1016/j.colsurfb.2005.07.014

757 Peris D et al. 2023. Macroevolutionary diversity of traits and genomes in the model yeast genus
758 Saccharomyces. Nat Commun. 14(1):690. https://doi.org/10.1038/s41467-023-36139-2

759 Peter J et al. 2018. Genome evolution across 1,011 Saccharomyces cerevisiae isolates. Nature.
760 556(7701):339–344. https://doi.org/10.1038/s41586-018-0030-5

761 Pinto J, Balarezo-Cisneros LN, Delneri D. 2025. Exploring adaptation routes to cold
762 temperatures in the Saccharomyces genus Peris D, editor. PLoS Genet. 21(2):e1011199.
763 https://doi.org/10.1371/journal.pgen.1011199

764 Piskur J et al. 2006. How did Saccharomyces evolve to become a good brewer? Trends in
765 Genetics. 22(4):183–186. https://doi.org/10.1016/j.tig.2006.02.002

766 Procházka E, Franko F, Poláková S, Sulo P. 2012. A complete sequence of *Saccharomyces*
767 *paradoxus* mitochondrial genome that restores the respiration in *S. cerevisiae*. FEMS Yeast
768 Res. 12(7):819–830. https://doi.org/10.1111/j.1567-1364.2012.00833.x

769 Quéméneur J-B et al. 2022. The relationships between growth rate and mitochondrial
770 metabolism varies over time. Sci Rep. 12(1):16066. https://doi.org/10.1038/s41598-022-20428-9

771 Rees JS, Castellano S, Andrés AM. 2020. The Genomics of Human Local Adaptation. Trends in
772 Genetics. 36(6):415–428. https://doi.org/10.1016/j.tig.2020.03.006

773 Reuß O, Vik Å, Kolter R, Morschhäuser J. 2004. The SAT1 flipper, an optimized tool for gene
774 disruption in Candida albicans. Gene. 341:119–127. https://doi.org/10.1016/j.gene.2004.06.021

775 Rikhvanov EG et al. 2001. [No title found]. Microbiology. 70(4):462–465.
776 https://doi.org/10.1023/A:1010442429489

777 Roop JI, Chang KC, Brem RB. 2016. Polygenic evolution of a sugar specialization trade-off in
778 yeast. Nature. 530(7590):336–339. https://doi.org/10.1038/nature16938

779 Roux F et al. 2016. Cytonuclear interactions affect adaptive traits of the annual plant
780 *Arabidopsis thaliana* in the field. Proc Natl Acad Sci USA. 113(13):3687–3692.
781 https://doi.org/10.1073/pnas.1520687113

782 Salminen TS, Vale PF. 2020. Drosophila as a Model System to Investigate the Effects of
783 Mitochondrial Variation on Innate Immunity. Front Immunol. 11:521.
784 https://doi.org/10.3389/fimmu.2020.00521

785 Salvadó Z et al. 2011. Temperature Adaptation Markedly Determines Evolution within the Genus
786 *Saccharomyces*. Appl Environ Microbiol. 77(7):2292–2302. https://doi.org/10.1128/AEM.01861-
787 10

788 Sánchez NS, Königsberg M. 2006. Using yeast to easily determine mitochondrial functionality
789 with 1-(4,5-dimethylthiazol-2-yl)-3,5-diphenyltetrazolium bromide (MTT) assay. Biochem
790 Molecular Bio Educ. 34(3):209–212. https://doi.org/10.1002/bmb.2006.49403403209

791 Serrano IM et al. 2024. Mitochondrial haplotype and mito-nuclear matching drive somatic
792 mutation and selection throughout ageing. Nat Ecol Evol. 8(5):1021–1034.
793 https://doi.org/10.1038/s41559-024-02338-3

794 Shoemaker M, Cohen I, Campbell M. 2004. Reduction of MTT by aqueous herbal extracts in the
795 absence of cells. Journal of Ethnopharmacology. 93(2–3):381–384.
796 https://doi.org/10.1016/j.jep.2004.04.011

797 Slater TF, Sawyer B, Sträuli U. 1963. Studies on succinate-tetrazolium reductase systems.
798 Biochimica et Biophysica Acta. 77:383–393. https://doi.org/10.1016/0006-3002(63)90513-4

799 Smukowski Heil C et al. 2021. Transposable Element Mobilization in Interspecific Yeast Hybrids
800 Vieira C, editor. Genome Biology and Evolution. 13(3):evab033.
801 https://doi.org/10.1093/gbe/evab033

802 Sork VL. 2017. Genomic Studies of Local Adaptation in Natural Plant Populations. Journal of
803 Heredity. 109(1):3–15. https://doi.org/10.1093/jhered/esx091

804 Starr TN, Thornton JW. 2016. Epistasis in protein evolution. Protein Science. 25(7):1204–1218.
805 https://doi.org/10.1002/pro.2897

806 Stern DB, Anderson NW, Diaz JA, Lee CE. 2022. Genome-wide signatures of synergistic
807 epistasis during parallel adaptation in a Baltic Sea copepod. Nat Commun. 13(1):4024.
808 https://doi.org/10.1038/s41467-022-31622-8

809 Sujkowski A et al. 2019. Mito-nuclear interactions modify Drosophila exercise performance.
810 Mitochondrion. 47:188–205. https://doi.org/10.1016/j.mito.2018.11.005

811 Sullivan LB, Chandel NS. 2014. Mitochondrial reactive oxygen species and cancer. Cancer
812 Metab. 2(1):17. https://doi.org/10.1186/2049-3002-2-17

813 Sulo P et al. 2003. The efficiency of functional mitochondrial replacement in species has
814 directional character. FEMS Yeast Research. 4(1):97–104. https://doi.org/10.1016/S1567-
815 1356(03)00109-0

816 Sun J et al. 2019. Mitochondrial variation in small brown planthoppers linked to multiple traits
817 and probably reflecting a complex evolutionary trajectory. Molecular Ecology. 28(14):3306–
818 3323. https://doi.org/10.1111/mec.15148

819 Swamy KBS et al. 2022. Proteotoxicity caused by perturbed protein complexes underlies hybrid
820 incompatibility in yeast. Nat Commun. 13(1):4394. https://doi.org/10.1038/s41467-022-32107-4

821 Sweeney J, Kuehne H, Sniegowski P. 2004. Sympatric natural and populations have different
822 thermal growth profiles. FEMS Yeast Research. 4(4–5):521–525. https://doi.org/10.1016/S1567-
823 1356(03)00171-5

824 Syenina A et al. 2020. Positive epistasis between viral polymerase and the 3′ untranslated
825 region of its genome reveals the epidemiologic fitness of dengue virus. Proc Natl Acad Sci USA.
826 117(20):11038–11047. https://doi.org/10.1073/pnas.1919287117

827 Tranah GJ. 2011. Mitochondrial–nuclear epistasis: Implications for human aging and longevity.
828 Ageing Research Reviews. 10(2):238–252. https://doi.org/10.1016/j.arr.2010.06.003

829 Tsai T, St. John JC. 2016. The role of mitochondrial DNA copy number, variants, and haplotypes
830 in farm animal developmental outcome. Domestic Animal Endocrinology. 56:S133–S146.
831 https://doi.org/10.1016/j.domaniend.2016.03.005

832 Vijayraghavan S et al. 2019. Mitochondrial Genome Variation Affects Multiple Respiration and
833 Nonrespiration Phenotypes in *Saccharomyces cerevisiae*. Genetics. 211(2):773–786.
834 https://doi.org/10.1534/genetics.118.301546

835 Wallace DC. 2015. Mitochondrial DNA Variation in Human Radiation and Disease. Cell.
836 163(1):33–38. https://doi.org/10.1016/j.cell.2015.08.067

837 Walunjkar N et al. 2025. Pervasive Divergence in Protein Thermostability is Mediated by Both
838 Structural Changes and Cellular Environments Zhang J, editor. Molecular Biology and Evolution.
839 42(7):msaf137. https://doi.org/10.1093/molbev/msaf137

840 Warringer J et al. 2011. Trait Variation in Yeast Is Defined by Population History Kruglyak L,
841 editor. PLoS Genet. 7(6):e1002111. https://doi.org/10.1371/journal.pgen.1002111

842 Weinreich DM, Watson RA, Chao L. 2005. Perspective: Sign epistasis and genetic constraint on
843 evolutionary trajectories. Evolution. 59(6):1165–1174

844 Weiss CV et al. 2018. Genetic dissection of interspecific differences in yeast thermotolerance.
845 Nat Genet. 50(11):1501–1504. https://doi.org/10.1038/s41588-018-0243-4

846 Weiss CV, Brem RB. 2019. Dissecting Trait Variation across Species Barriers. Trends in
847 Ecology & Evolution. 34(12):1131–1136. https://doi.org/10.1016/j.tree.2019.07.013

848 Wolff JN, Ladoukakis ED, Enríquez JA, Dowling DK. 2014. Mitonuclear interactions:
849 evolutionary consequences over multiple biological scales. Philos Trans R Soc Lond B Biol Sci.
850 369(1646):20130443. https://doi.org/10.1098/rstb.2013.0443

851 Wolters JF et al. 2018. Mitochondrial Recombination Reveals Mito–Mito Epistasis in Yeast.
852 Genetics. 209(1):307–319. https://doi.org/10.1534/genetics.117.300660

853 Wolters JF, Chiu K, Fiumera HL. 2015. Population structure of mitochondrial genomes in
854 Saccharomyces cerevisiae. BMC Genomics. 16(1):451. https://doi.org/10.1186/s12864-015-
855 1664-4

856 Yang L-L, Tang S-K, Huang Y, Zhi X-Y. 2015. Low Temperature Adaptation Is Not the Opposite
857 Process of High Temperature Adaptation in Terms of Changes in Amino Acid Composition.
858 Genome Biol Evol. 7(12):3426–3433. https://doi.org/10.1093/gbe/evv232

859

860

Fig 1

(A)

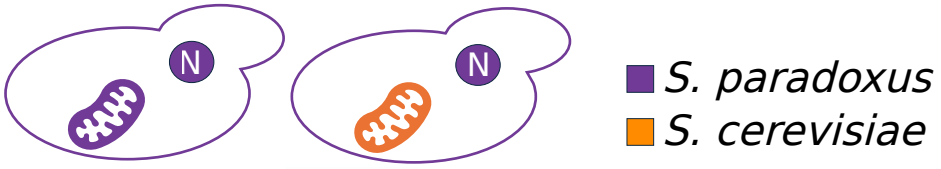
N
N
S. paradoxus
S. cerevisiae

(B)

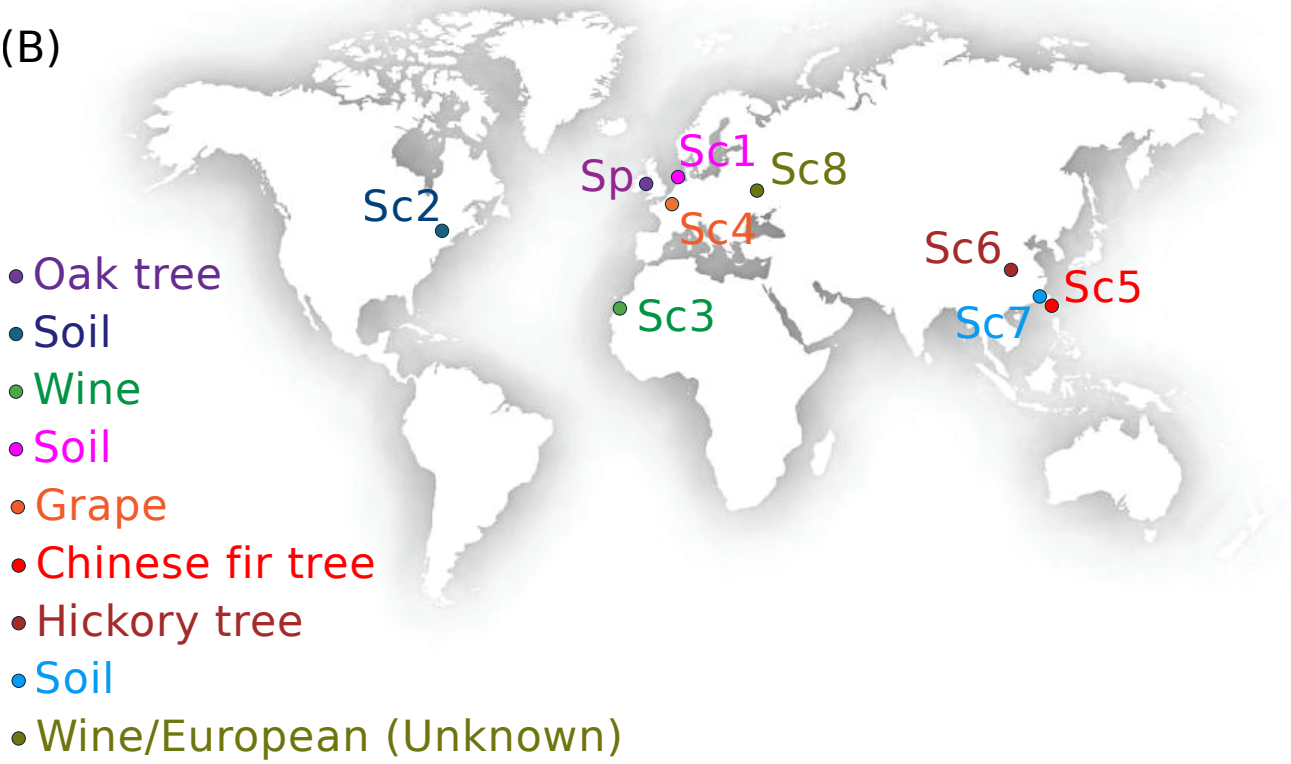
Sp
Sc1
Sc8
Sc2
Sc4
Sc6
Sc5
Sc3
Sc7
Oak tree
Soil
Wine
Soil
Grape
Chinese fir tree
Hickory tree
Soil
Wine/European (Unknown)

Fig. 2

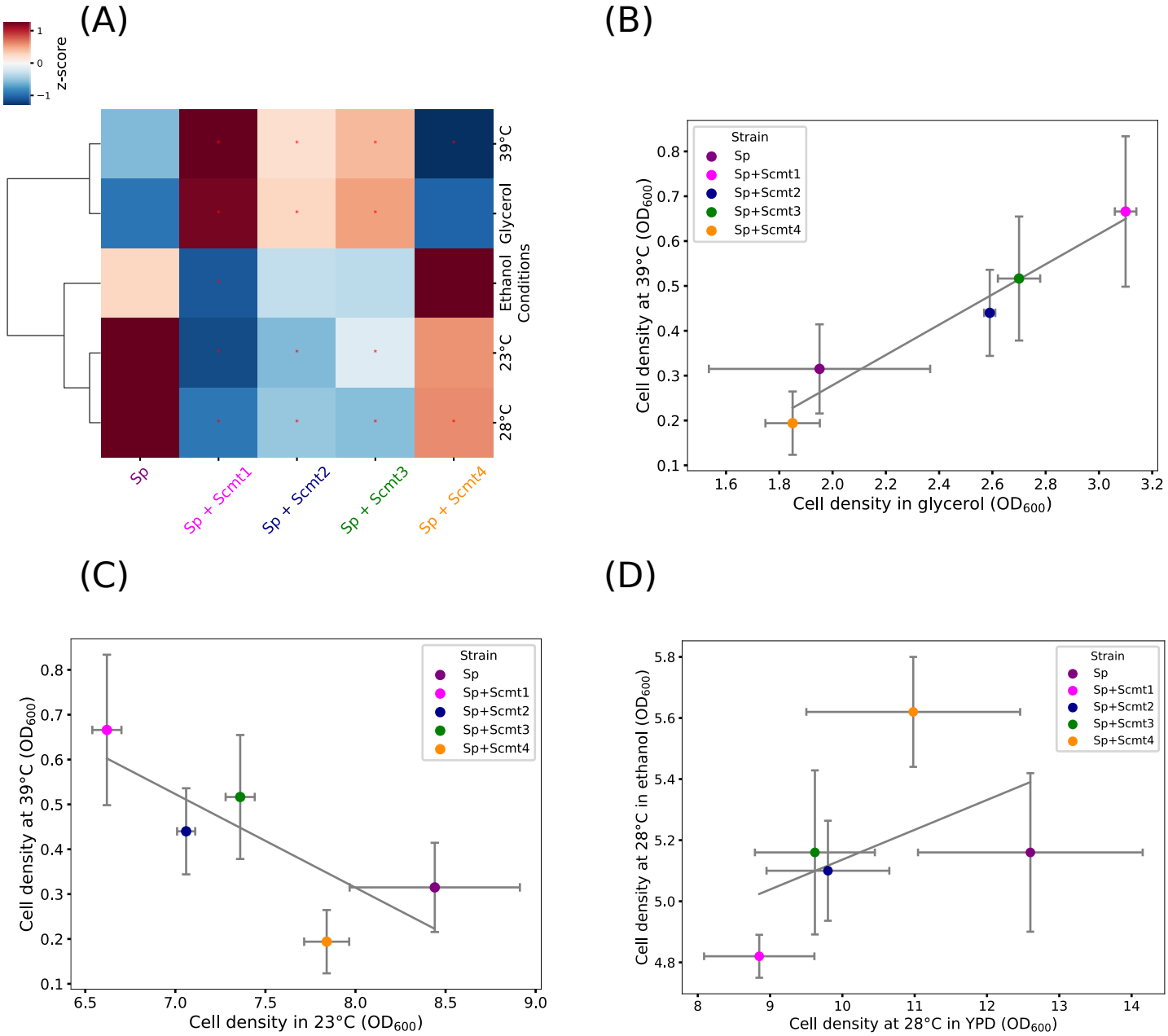
(A)
z-score
1
0
−1
39°C
Glycerol
Ethanol
23°C
28°C
Conditions
Sp
Sp + Scmt1
Sp + Scmt2
Sp + Scmt3
Sp + Scmt4
(B)
Strain
Sp
Sp+Scmt1
Sp+Scmt2
Sp+Scmt3
Sp+Scmt4
Cell density at 39°C (OD600)
Cell density in glycerol (OD600)
(C)
Strain
Sp
Sp+Scmt1
Sp+Scmt2
Sp+Scmt3
Sp+Scmt4
Cell density at 39°C (OD600)
Cell density in 23°C (OD600)
(D)
Strain
Sp
Sp+Scmt1
Sp+Scmt2
Sp+Scmt3
Sp+Scmt4
Cell density at 28°C in ethanol (OD600)
Cell density at 28°C in YPD (OD600)

Fig. 3

(A)

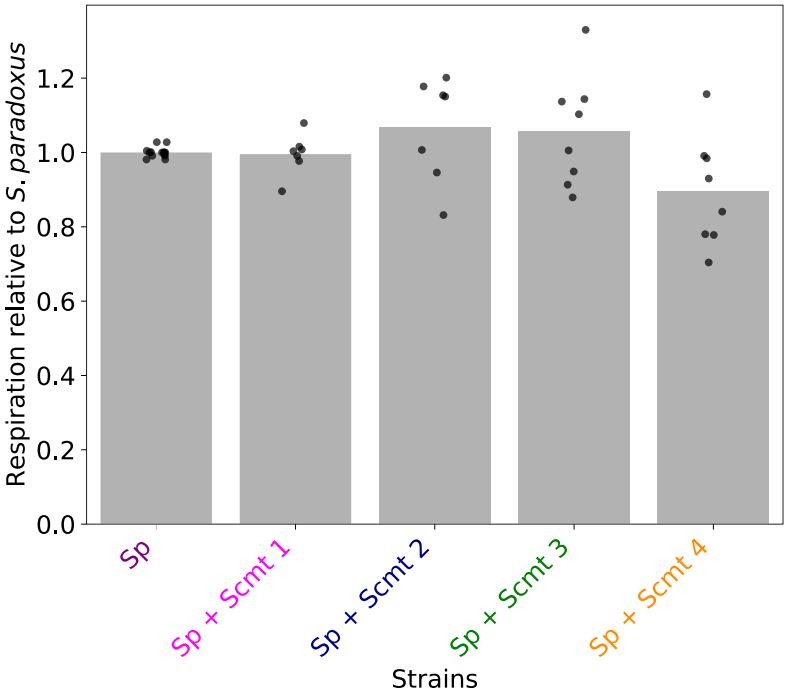
Respiration relative to S. paradoxus
0.0
0.2
0.4
0.6
0.8
1.0
1.2
Sp
Sp + Scmt 1
Sp + Scmt 2
Sp + Scmt 3
Sp + Scmt 4
Strains

(B)

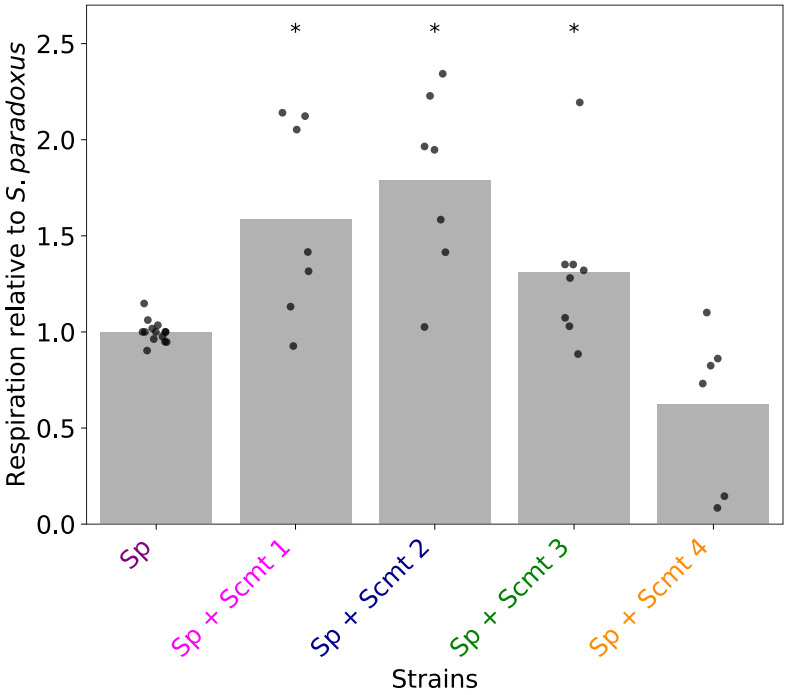
Respiration relative to S. paradoxus
0.0
0.5
1.0
1.5
2.0
2.5
*
*
*
Sp
Sp + Scmt 1
Sp + Scmt 2
Sp + Scmt 3
Sp + Scmt 4
Strains

Fig. 4

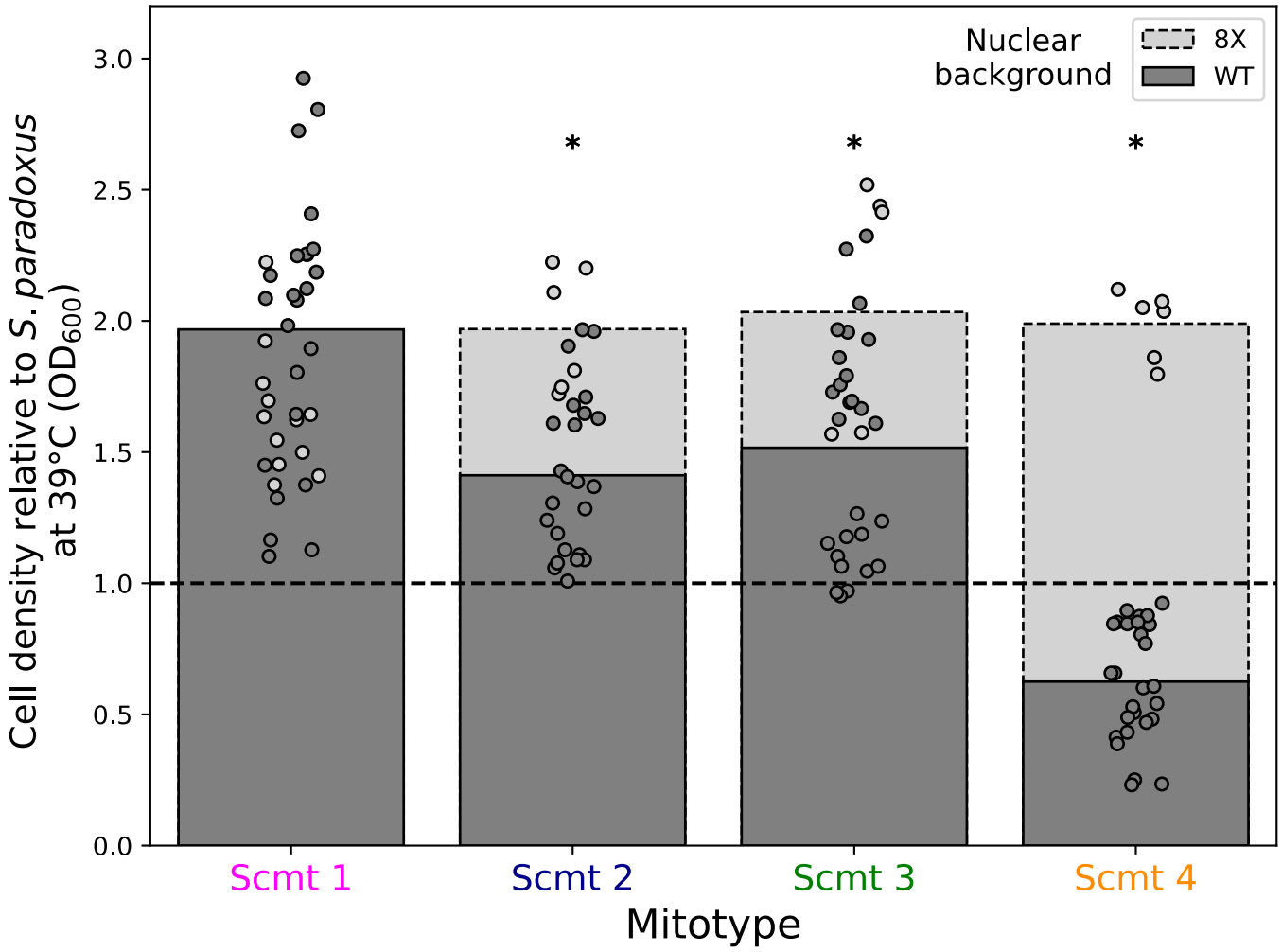
Nuclear background
8X
WT
Cell density relative to S. paradoxus at 39°C (OD600)
3.0
2.5
2.0
1.5
1.0
0.5
0.0
*
*
*
Scmt 1
Scmt 2
Scmt 3
Scmt 4
Mitotype